

Wireless Network Cocast: Location-Aware Cooperative Communications with Linear Network Coding

Hung-Quoc Lai, Ahmed S. Ibrahim[†], and K. J. Ray Liu[†]

US Army RDECOM CERDEC, AMSRD-CER-ST-WL-NS,
Meyer Center, Ft. Monmouth, NJ 07703, USA.

Email: hungquoc.lai@us.army.mil

[†]Department of Electrical and Computer Engineering
University of Maryland, College Park, MD 20742, USA.

Email: {asalah, kjrlui}@umd.edu

Abstract

In wireless networks, reducing aggregate transmit power and in many cases, having even power distribution increase the network lifetime. Conventional direct transmission (DTX) scheme results in high aggregate transmit power and uneven power distribution. In this paper, we consider location-aware cooperation-based schemes namely immediate-neighbor cooperation (INC), maximal cooperation (MAX), and wireless network cocast (WNC) that achieve spatial diversity to reduce aggregate transmit power and even power distribution. INC utilizes two-user cooperative communication, resulting in good reduction of aggregate transmit power and low transmission delay; however, power distribution is still uneven. MAX utilizes multi-node cooperative communication, providing *incremental diversity* to achieve even power distribution and substantial reduction in aggregate transmit power. Transmission delay in MAX, however, grows quadratically with network sizes. As a result, the novel WNC is proposed to achieve incremental diversity as in MAX and low transmission delay as in INC. In WNC, mobile units acting as relays form unique linearly-coded signals from overheard signals and transmit them to the destination, where a multiuser detector jointly detects the symbols from all received signals. Performance evaluation in uniformly distributed networks shows that INC, MAX, and WNC substantially reduce aggregate transmit power while MAX and WNC also provide even power distribution.

Keywords: Location-aware, cooperative communication, incremental diversity, cocast, amplify-and-forward, decode-and-forward, multiuser detection.

Report Documentation Page				Form Approved OMB No. 0704-0188	
Public reporting burden for the collection of information is estimated to average 1 hour per response, including the time for reviewing instructions, searching existing data sources, gathering and maintaining the data needed, and completing and reviewing the collection of information. Send comments regarding this burden estimate or any other aspect of this collection of information, including suggestions for reducing this burden, to Washington Headquarters Services, Directorate for Information Operations and Reports, 1215 Jefferson Davis Highway, Suite 1204, Arlington VA 22202-4302. Respondents should be aware that notwithstanding any other provision of law, no person shall be subject to a penalty for failing to comply with a collection of information if it does not display a currently valid OMB control number.					
1. REPORT DATE 2009		2. REPORT TYPE		3. DATES COVERED 00-00-2009 to 00-00-2009	
4. TITLE AND SUBTITLE Wireless Network Cocast: Location-Aware Cooperative Communications with Linear Network Coding				5a. CONTRACT NUMBER	
				5b. GRANT NUMBER	
				5c. PROGRAM ELEMENT NUMBER	
6. AUTHOR(S)				5d. PROJECT NUMBER	
				5e. TASK NUMBER	
				5f. WORK UNIT NUMBER	
7. PERFORMING ORGANIZATION NAME(S) AND ADDRESS(ES) US Army RDECOM CERDEC,AMSRD-CER-ST-WL-NS,Meyer Center,Fort Monmouth,NJ,07703				8. PERFORMING ORGANIZATION REPORT NUMBER	
9. SPONSORING/MONITORING AGENCY NAME(S) AND ADDRESS(ES)				10. SPONSOR/MONITOR'S ACRONYM(S)	
				11. SPONSOR/MONITOR'S REPORT NUMBER(S)	
12. DISTRIBUTION/AVAILABILITY STATEMENT Approved for public release; distribution unlimited					
13. SUPPLEMENTARY NOTES IEEE Trans. on Wireless Communications					
14. ABSTRACT see report					
15. SUBJECT TERMS					
16. SECURITY CLASSIFICATION OF:			17. LIMITATION OF ABSTRACT Same as Report (SAR)	18. NUMBER OF PAGES 28	19a. NAME OF RESPONSIBLE PERSON
a. REPORT unclassified	b. ABSTRACT unclassified	c. THIS PAGE unclassified			

1 Introduction

In conventional direct transmission (DTX), where mobile units directly transmit their information to a common destination, the distant mobile units require more transmit power to provide a comparable quality of service (QoS) to that of the closer ones. Consequently, high aggregate transmit power, which is the sum of all transmit power of individual mobile units, and uneven power distribution among them exist in the network. These two issues result in low network lifetime, which is defined in this paper as the time until the first mobile unit dies. It is well-known that diversity techniques such as time diversity, frequency diversity, and spatial diversity result in reduction of transmit power and thus can be used to improve network lifetime. Among these techniques, spatial diversity achieved by cooperative communication [1], [2] has recently been studied.

Cooperative communication makes use of broadcast nature of wireless transmission. Nodes in a network acting as relays can retransmit overheard information to a destination, where the intended information from the source signal and the relay signals is jointly detected. The distributed antennas among the relays are used to provide spatial diversity without the need to use multiple antennas at the source. Various cooperative diversity protocols have been proposed and analyzed in [3]-[8]. Decode-and-forward (DAF) and amplify-and-forward (AAF) protocols for cooperative communication are explained in [3]. In DAF protocol, each relay decodes the overheard information from the source, re-encodes it, and then forwards it to the destination. In AAF protocol, each relay simply amplifies the overheard signal and forwards it to the destination. Symbol error rate (SER) for single- and multi-node DAF protocol was analyzed in [4] and [5], respectively. In [6] and [7], various relay selection schemes have been proposed that achieve high bandwidth efficiency and full diversity order. Finally, distributed space time codes for DAF and AAF protocols have been proposed and analyzed in [8].

Much research in cooperative communication has considered symmetric problems, in which a pair of nodes help each other in their transmission to a common destination [9]-[13], or different source nodes in a network receive assistance from the same group of relays to achieve the same diversity order [14]. However, practical networks are asymmetric in nature. Node distances to a common destination vary based on node locations, and thus some nodes are disadvantageous in their transmission in comparison with others. Therefore, the node locations, which can be obtained using

network-aided position techniques [15], [16], should be taken into consideration to improve network performance. In this work, we consider a number of location-aware cooperation-based schemes that achieve spatial diversity to reduce aggregate transmit power and achieve even power distribution in a network, where mobile units with known locations transmit their information to a common destination. The first proposed scheme, namely immediate-neighbor cooperation (INC), utilizes two-user cooperative communication [4] in a network. In INC, each mobile unit, except the closest node to the destination, is assigned a single relay, its immediate neighbor toward the destination, and thus a fixed diversity order of two is achieved. Consequently, INC achieves good reduction in aggregate transmit power with the expense of $(2N - 1)$ time slots for a network of N mobile units. However, distant users still require more power than the closer ones and power distribution is still uneven as in DTX.

The fundamental cause of high aggregate transmit power and uneven power distribution attributes to the dependency of transmit power on the distance between the source and the destination. Therefore, *incremental diversity*, a measure of diversity order of mobile units that varies incrementally in terms of node location, should be leveraged in a network to provide high diversity orders for distant units to compensate the high required transmit power. The second proposed scheme, namely maximal cooperation (MAX), provides incremental diversity to a network by means of cooperative communication. Multi-node cooperative communication [5] is utilized in MAX, where each mobile unit is assigned a group of mobile units locating between itself and the destination as relays. Thus the more distant the mobile unit, the higher diversity order to compensate the high required transmit power. Furthermore, the higher transmit power is shared and compensated by the larger group of relaying mobile units. Consequently, MAX with the incremental diversity achieves great reduction of aggregate transmit power and even power distribution.

The major drawback in MAX is the large transmission delay since each relay requires a time slot for its transmission. For a network of N mobile units, MAX incurs a delay of $N(N + 1)/2$ time slots, which grows quadratically with the network size, defined as the number of mobile units N . Therefore, our main focus in this work is to introduce a novel concept of wireless network cocast¹ (WNC) to resolve the weaknesses of INC and MAX. Cocast, an analogy to broadcast, unicast, and

¹*cocast* \equiv *cooperative cast*

multicast, is a newly defined transmission method that utilizes linear network coding for a number of nodes to cooperatively transmit their information to the same intended destination. WNC achieves the incremental diversity as in MAX with the low transmission delay of $(2N - 1)$ time slots as in INC. Both DAF and AAF protocols in cooperative communication are considered in WNC, where mobile units acting as relays form unique linearly-coded signals from a set of overheard symbols of different sources and transmit them to the destination. At the destination, a multiuser detection technique jointly detects the intended symbols from all received signals in the network. We derive the exact and the asymptotic symbol-error-rate (SER) expressions² for general M-PSK modulation for DAF WNC protocol. The extension to general M-QAM can follow directly. For AAF WNC protocol, we offer the conditional SER expression given the channel knowledge. Performance evaluation in uniformly distributed networks shows that INC, MAX, and WNC outperform DTX greatly in terms of aggregate transmit power and power distribution. Furthermore, WNC achieves low aggregate transmit power and even power distribution of MAX with low transmission delay of INC.

The rest of this paper is organized as follows. After this introduction section, the transmission structure of DAF and AAF WNC protocols is introduced in Section 2. Multiuser detection used in WNC is presented in Section 3 for both DAF and AAF WNC protocols. The performance analysis is presented in Section 4 to provide the exact and the asymptotic SER expressions for DAF WNC protocol and the conditional SER expression for AAF WNC protocol. Simulation for BPSK modulation is provided to validate the SER performance of DAF and AAF WNC protocols. In Section 5, expressions of aggregate transmit power and power distribution in a network and the transmission delay for DTX, INC, MAX, and WNC are derived for BPSK modulation using the asymptotic SER expressions. These expressions then are used to provide performance evaluation of INC, MAX, and WNC over DTX in Section 6. In this section, performance evaluation is also provided to verify that WNC can achieve the low aggregate transmit power and power distribution of MAX with the low transmission delay of INC. Lastly, we draw some conclusions in Section 7.

²Asymptotic SER performance is a performance at high signal-to-noise ratio.

2 WNC with Linear Network Coding

We consider a wireless network consisting of a destination d and N mobile units U_1, U_2, \dots, U_N as shown in Figure 1. The mobile units are located within an area $\mathcal{A} \in \mathbb{R}_+^2$ at distances d_1, d_2, \dots, d_N to the destination while the destination is at $(0,0)$. Without loss of generality, the mobile units are numbered in decreasing order of their distance to the destination. In this manner, U_1 and U_N are the farthest and the closest to d , respectively. These mobile units U_1, U_2, \dots, U_N possess their own information represented by symbols x_1, x_2, \dots, x_N , respectively, that need to be delivered to d . Channels among the mobile units and the destination are modeled as narrow-band Rayleigh fading with additive white Gaussian noise (AWGN). Let h_{uv} denote a generic channel coefficient representing the channel between any two nodes. Then h_{uv} is modeled as a zero-mean circular symmetric complex Gaussian random variable with variance $\sigma_{uv}^2 = d_{uv}^{-\alpha}$, where d_{uv} is the distance between the two nodes and α is the path loss exponent. The transmission from the mobile units is subject to time-division multiple access (TDMA), and we expect the same QoS, which can be represented by a SER p_0 , in delivering x_1, x_2, \dots, x_N to d .

Figure 2 illustrates the WNC transmission structure, in which each mobile unit U_i for $i = 2, 3, \dots, N$ is allocated two time slots. In the first time slot, U_i acting as a relay node forms a unique linearly-coded signal, a linear combination of a set of overheard symbols x_1, \dots, x_{i-1} , and transmits it to d . U_i can either decode the overheard signals and re-encode the symbols, the so-called DAF WNC protocol, or simply amplify the overheard signals, the so-called AAF WNC protocol. In the second time slot, U_i acting as a source node transmits its own symbol x_i to U_{i+1}, \dots, U_N and d . U_1 has one time slot for its own transmission since it is not required to assist other nodes. The total time slots required to transmit a set of N symbols is $2N - 1$, among which N time slots for source transmission and $N - 1$ time slots for relay transmission. The transmit power P_j associated with symbol x_j is distributed among the source node and the corresponding relay nodes. We have $P_j = \sum_{i=j}^N P_{ij}$, where P_{ij} is the power from U_i in transmitting x_j . Because the destination detects symbol x_j based on $N - j + 1$ copies of the symbol, we expect spatial diversity orders of $N, N - 1, \dots, 1$ for x_1, x_2, \dots, x_N , respectively, which will be verified later in the paper.

To eliminate interference in the linearly coded version of the overheard symbols, each symbol x_j

is protected by a signature waveform $s_j(t)$, where $\|s_j(t)\|^2 = 1$. The cross-correlation between $s_j(t)$ and $s_i(t)$ is $\rho_{ji} = \langle s_j(t), s_i(t) \rangle$, where $\langle f(t), g(t) \rangle \triangleq \int_0^T f(t)g^*(t)dt$ is the inner product between $f(t)$ and $g(t)$ with the symbol interval T and $*$ representing the complex conjugate. We assume that each mobile unit also knows the signature waveforms of others. In the sequel, we will present in detail the system model in DAF and AAF WNC protocols.

2.1 DAF WNC Protocol

In DAF WNC protocol, U_i in its first time slot decodes the overheard symbol and includes the symbol in its transmission only if the decoding is successful [4],[5]. The received signals at the destination from U_i in its first time slot is

$$y_{idr}^D(t) = h_{id} \sum_{j=1}^{i-1} \sqrt{\tilde{P}_{ij}^D} x_j s_j(t) + n_{idr}^D(t), \quad (1)$$

for $i = 2, \dots, N$ and $j = 1, \dots, i-1$, where

$$\tilde{P}_{ij}^D = \begin{cases} P_{ij} & \text{if } U_i \text{ decodes } x_j \text{ correctly} \\ 0 & \text{otherwise} \end{cases}. \quad (2)$$

We defer the discussion of detection at mobile units acting as relays and power allocation among cooperative nodes to Sections 3 and 4.2, respectively. The received signals at the destination from U_i in the second time slot is

$$y_{ido}^D(t) = \sqrt{P_{ii}} h_{id} x_i s_i(t) + n_{ido}^D(t). \quad (3)$$

In (1) and (3), $n_{idr}^D(t)$ and $n_{ido}^D(t)$ are modeled as independent and identically-distributed (i.i.d.) zero-mean AWGN with variance N_0 . Note that the signal from U_1 follows (3) with $i = 1$ since it transmits its own symbol only. Note further that in the second time slot, other mobile units U_k for $k = i+1, \dots, N$ also receive the signal from U_i as

$$y_{iko}(t) = \sqrt{P_{ii}} h_{ik} x_i s_i(t) + n_{iko}^D(t). \quad (4)$$

For notational convenience, we denote $a_{ij}^D = \sqrt{\tilde{P}_{ij}^D} h_{id}$ and $a_{ii}^D = \sqrt{P_{ii}} h_{id}$ as signal coefficients and rewrite (1) and (3) as

$$y_{idr}^D(t) = \sum_{j=1}^{i-1} a_{ij}^D x_j s_j(t) + n_{idr}^D(t) \quad (5)$$

and

$$y_{ido}^D(t) = a_{ii}^D x_i s_i(t) + n_{ido}^D(t), \quad (6)$$

respectively.

2.2 AAF WNC Protocol

The difference between AAF and DAF protocols is that U_i simply amplifies the overheard signals and forwards a linearly coded version of these signals to d in its first time slot. In this time slot, the received signals at the destination is

$$y_{idr}^A(t) = h_{id} \sum_{j=1}^{i-1} \frac{\sqrt{P_{ij}}}{\sqrt{P_{jj}|h_{ji}|^2 + N_0}} y_{jio}(t) + n_{idr}^A(t), \quad (7)$$

where

$$y_{jio}^A(t) = \sqrt{P_{jj}} h_{ji} x_j s_j(t) + n_{jio}^A(t), \quad (8)$$

is the received signal at relay i corresponding to transmit symbol x_j for $i = 1, \dots, N$ and $j = 1, \dots, i-1$.

The received signal at the destination from U_i in its second time slot is

$$y_{ido}^A(t) = \sqrt{P_{ii}} h_{id} x_i s_i(t) + n_{ido}^A(t). \quad (9)$$

In (7)-(9), $n_{idr}^A(t)$, $n_{jio}^A(t)$, and $n_{ido}^A(t)$ are modeled as i.i.d. zero-mean AWGN with variance N_0 . The signal from U_1 follows (9) with $i = 1$. As in the case of DAF, other mobile units U_k for $k = i+1, \dots, N$ also receive the signal from U_i in the second time slot as

$$y_{iko}(t) = \sqrt{P_{ii}} h_{ik} x_i s_i(t) + n_{iko}^A(t). \quad (10)$$

Substituting (8) into (7), we have

$$\begin{aligned} y_{idr}^A(t) &= h_{id} \sum_{j=1}^{i-1} \frac{\sqrt{P_{ij} P_{jj}} h_{ji}}{\sqrt{P_{jj}|h_{ji}|^2 + N_0}} x_j s_j(t) + h_{id} \sum_{j=1}^{i-1} \frac{\sqrt{P_{ij}}}{\sqrt{P_{jj}|h_{ji}|^2 + N_0}} n_{jio}(t) + n_{idr}^A(t) \\ &= \sum_{j=1}^{i-1} a_{ij}^A x_j s_j(t) + \tilde{n}_{idr}^A(t), \end{aligned} \quad (11)$$

where we denote $a_{ij}^A = \sqrt{\tilde{P}_{ij}^A} h_{id}$, in which

$$\tilde{P}_{ij}^A = \frac{P_{ij} P_{jj} |h_{ji}|^2}{P_{jj} |h_{ji}|^2 + N_0}, \quad (12)$$

as a signal coefficient from U_i in association with x_j . The resulting noise $\tilde{n}_{idr}^A(t)$ has power spectral density $N_0 f_i$, where

$$f_i = \sum_{j=1}^{i-1} \frac{P_{ij}|h_{id}|^2}{P_{jj}|h_{ji}|^2 + N_0} + 1 \quad (13)$$

is a factor representing the noise amplification impact at U_i . Likewise, we denote $a_{ii}^A = \sqrt{P_{ii}}h_{id}$ and rewrite (9) as

$$y_{ido}^A(t) = a_{ii}^A x_i s_i(t) + n_{ido}^A(t). \quad (14)$$

2.3 A General System Model for WNC Protocols

We see that DAF and AAF WNC protocols share the same system model with different parameters. For notational convenience in subsequent analysis, we denote the transmit signals from U_i in the first and the second time slots as

$$y_{idr}(t) = \sum_{j=1}^{i-1} a_{ij} x_j s_j(t) + n_{idr}(t) \quad (15)$$

and

$$y_{ido}(t) = a_{ii} x_i s_i(t) + n_{ido}(t), \quad (16)$$

respectively, for $i = 1, \dots, N$ and $j = 1, \dots, i-1$. In the above equations, $a_{ii} = \sqrt{P_{ii}}h_{id}$, $a_{ij} = \sqrt{\tilde{P}_{ij}}h_{id}$ where \tilde{P}_{ij} follows (2) and (12) for DAF and AAF, respectively, and the power spectral density of $n_{ido}(t)$ and $n_{idr}(t)$ is N_0 and $N_0 f_i$, respectively with

$$f_i = \begin{cases} 1 & \text{for DAF} \\ \sum_{j=1}^{i-1} \frac{P_{ij}|h_{id}|^2}{P_{jj}|h_{ji}|^2 + N_0} + 1 & \text{for AAF} \end{cases} \quad (17)$$

3 Signal Detection in WNC

Since we assume each mobile unit knows the signature waveforms of other mobile units, the detection of symbol x_j at mobile unit U_i for $j = 1, \dots, N$ and $i = j+1, \dots, N$ in DAF WNC protocol follows matched-filtering that is applied to the received signal $y_{jio}^D(t)$ as

$$\hat{x}_{ji} \triangleq \langle y_{jio}^D(t), s_j(t) \rangle = \sqrt{P_{jj}}h_{ji}x_j + n_{ji}, \quad (18)$$

where $n_{ji} \sim \mathcal{N}(0, N_0)$. Here no multiuser detection is required at mobile units.

Signal detection at the destination in DAF and AAF WNC protocols is performed by first applying matched-filtering to the received signals with respect to signature waveforms. Then multiuser detection is followed to obtain a set of desired symbols. In the sequel, we explain these steps in detail.

3.1 Matched Filtering

Given the system models in Section 2, the destination receives N direct transmissions in the odd time slots and $(N-1)$ relaying transmissions in the even ones. Matched-filtering with respect to signature waveforms is applied to the received signals to produce a total of $M = \frac{N(N+1)}{2}$ discrete-time signals of the forms

$$y_{idj} = \langle y_{idr}(t), s_j(t) \rangle = a_{ij}x_j + \sum_{\substack{k=1 \\ k \neq j}}^{i-1} a_{ik}\rho_{jk}x_k + n_{idj} \quad (19)$$

and

$$y_{idi} = \langle y_{ido}(t), s_i(t) \rangle = a_{ii}x_i + n_{idi} \quad (20)$$

for $i = 1, \dots, N$ and $j = 1, \dots, i-1$. In (19) and (20), $n_{idi} \sim \mathcal{N}(0, N_0)$ and $n_{idj} \sim \mathcal{N}(0, N_0 f_i)$ are the AWGN.

Let $\mathbf{y} = [y_{1d1}, y_{2d1}, y_{2d2}, \dots, y_{id1}, \dots, y_{idj}, \dots, y_{idi}, \dots, y_{Nd1}, \dots, y_{NdN}]^T$, where T denotes transpose, be the $M \times 1$ received signal vector and $\mathbf{R}_i = \langle \mathbf{s}_i, \mathbf{s}_i^H \rangle$ be the cross-correlation matrix where $\mathbf{s}_i = [s_1(t), s_2(t), \dots, s_i(t)]^T$. We can write

$$\mathbf{y} = \mathbf{R}\mathbf{A}\mathbf{x} + \mathbf{n}, \quad (21)$$

where $\mathbf{x} = [x_1, x_2, \dots, x_N]^T$ is the $N \times 1$ transmit symbol vector,

$$\mathbf{R} = \text{diag}\{1, \mathbf{R}_1, 1, \mathbf{R}_2, 1, \dots, \mathbf{R}_{i-1}, 1, \dots, \mathbf{R}_{N-1}, 1\}$$

is the $M \times M$ cross-correlation matrix, and

$$\mathbf{A} = \begin{bmatrix} \text{diag}(a_{11}) & \mathbf{0}_{1 \times (N-1)} \\ \text{diag}(a_{21}, a_{22}) & \mathbf{0}_{2 \times (N-2)} \\ \text{diag}(a_{31}, a_{32}, a_{33}) & \mathbf{0}_{3 \times (N-3)} \\ \vdots & \vdots \\ \text{diag}(a_{i1}, \dots, a_{ij}, \dots, a_{ii}) & \mathbf{0}_{i \times (N-i)} \\ \vdots & \vdots \\ \text{diag}(a_{N1}, \dots, a_{Nj}, \dots, a_{NN}) & \vdots \end{bmatrix}$$

is the $M \times N$ signal coefficient matrix. In the above equations, $\text{diag}\{.\}$ and $\mathbf{0}_{u \times v}$ denote a diagonal matrix and a u -by- v matrix of zeros, respectively. Also in (21), $\mathbf{n} \sim \mathcal{N}(\mathbf{0}, N_0 \tilde{\mathbf{R}})$ where $\mathbf{0}$ is an $M \times 1$ vector of zeros and

$$\tilde{\mathbf{R}} = \text{diag} \left\{ 1, \tilde{\mathbf{R}}_1, 1, \tilde{\mathbf{R}}_2, 1, \dots, \tilde{\mathbf{R}}_{i-1}, 1, \dots, \tilde{\mathbf{R}}_{N-1}, 1 \right\}$$

with $\tilde{\mathbf{R}}_{i-1} = f_i \mathbf{R}_{i-1}$. Let us define

$$\mathbf{F} \triangleq \text{diag} \left\{ 1, f_2, 1, f_3, f_3, 1, \dots, \underbrace{f_i, \dots, f_i}_{(i-1) \text{ times}}, 1, \dots, \underbrace{f_N, \dots, f_N}_{(N-1) \text{ times}}, 1 \right\},$$

then $\tilde{\mathbf{R}} = \mathbf{F}\mathbf{R}$ and $\mathbf{n} \sim \mathcal{N}(\mathbf{0}, N_0 \mathbf{F}\mathbf{R})$.

3.2 Multiuser Detection Scheme

Assume \mathbf{R}_i is invertible with the invert matrix \mathbf{R}_i^{-1} . Then the inverse of \mathbf{R} exists with $\mathbf{R}^{-1} = \text{diag} \{1, \mathbf{R}_1^{-1}, 1, \mathbf{R}_2^{-1}, 1, \dots, \mathbf{R}_{i-1}^{-1}, 1, \dots, \mathbf{R}_{N-1}^{-1}, 1\}$. Multiuser detection is applied to the received signal vector in two steps. First the vector \mathbf{y} is pre-multiplied with the inverse \mathbf{R}^{-1} to obtain

$$\tilde{\mathbf{y}} = \mathbf{R}^{-1} \mathbf{y} = \mathbf{A}\mathbf{x} + \tilde{\mathbf{n}}, \quad (22)$$

where $\tilde{\mathbf{n}} \sim \mathcal{N}(\mathbf{0}, N_0 \mathbf{R}^{-1} \mathbf{F})$. Then $\tilde{\mathbf{y}}$ is grouped into $(N - j + 1) \times 1$ signal vectors in association with the desired symbols x_j as

$$\mathbf{y}_j = \mathbf{a}_j x_j + \mathbf{n}_j, \quad (23)$$

where $\mathbf{a}_j = [a_{jj}, \dots, a_{ij}, \dots, a_{Nj}]^T$ for $j = 1, \dots, N$ and $i = j, \dots, N$ and $\mathbf{n}_j \sim \mathcal{N}(\mathbf{0}, \mathbf{K}_j)$. We have $\mathbf{K}_j = \text{diag} \{ \sigma_{jj}^2, \dots, \sigma_{ij}^2, \dots, \sigma_{Nj}^2 \}$, where

$$\sigma_{ij}^2 = N_0 \begin{cases} 1 & \text{if } i = j \\ f_i r_{ij} & \text{if } j < i \leq N \end{cases}. \quad (24)$$

In (24), f_i follows (17) and $r_{ij} \triangleq (\mathbf{R}_{i-1}^{-1})_{jj}$ represents the interference impact on the symbol x_j in the linearly-coded signal of overheard symbols from U_i . For the case of $\rho_{ji} = \rho$ for all $i \neq j$, it can be shown [17] that

$$r_{ij} = \frac{1 + (i - 3)\rho}{(1 - \rho)(1 + (i - 2)\rho)} \triangleq r_i, \quad (25)$$

independent of j . Now let us define

$$\mathbf{b}_j \triangleq \left[\frac{a_{jj}}{\sigma_{jj}^2}, \dots, \frac{a_{ij}}{\sigma_{ij}^2}, \dots, \frac{a_{Nj}}{\sigma_{Nj}^2} \right]^T. \quad (26)$$

Then the desired symbol is detected based on

$$\hat{x}_j \triangleq \mathbf{b}_j^H \mathbf{y}_j = a_j x_j + n_j, \quad (27)$$

where $a_j \triangleq \mathbf{b}_j^H \mathbf{a}_j = \sum_{i=j}^N \frac{|a_{ij}|^2}{\sigma_{ij}^2}$, and $n_j \triangleq \mathbf{b}_j^H \mathbf{n}_j \sim \mathcal{N}(0, \sigma_j^2)$ with $\sigma_j^2 = \sum_{i=j}^N \frac{|a_{ij}|^2}{\sigma_{ij}^2}$.

4 Performance Analysis of WNC

The detection in (27) provides the maximal conditional signal-to-interference-plus-noise ratio (SINR) γ_j corresponding to the desired symbol x_j as

$$\gamma_j = \frac{a_j^2}{\sigma_j^2} = \sum_{i=j}^N \frac{|a_{ij}|^2}{\sigma_{ij}^2} = \frac{P_{jj}|h_{jd}|^2}{N_0} + \sum_{i=j+1}^N \frac{\tilde{P}_{ij}|h_{id}|^2}{f_i r_{ij} N_0}. \quad (28)$$

In the sequel, we derive the exact and the asymptotic SER expressions for the use of M-PSK modulation in DAF WNC protocol; a similar approach can be used to obtain SER expressions for the case of M-QAM modulation. We also provide simulations to validate the SER performance of both DAF and AAF WNC protocols.

4.1 SER Expression for WNC Protocol

For DAF WNC protocol, let $\beta_{ij} \in \{0, 1\}$ for $j = 1, \dots, (N-1)$ and $i = j+1, \dots, N$ represent a success or a failure in detection of x_j at U_i . Because U_i forwards x_j only if it has successfully detected the symbol, $\tilde{P}_{ij} = P_{ij}\beta_{ij}$. All β_{ij} 's form a decimal number $S_j = \sum_{i=j+1}^N \beta_{ij} 2^{N-i}$, which represents one of $2^{(N-j)}$ detection states of $(N-j)$ mobile units U_{j+1}, \dots, U_N acting as relays in association with x_j . Because the detection is independent from one mobile unit to the other, β_{ij} 's are independent Bernoulli random variables with a distribution

$$G(\beta_{ij}) = \begin{cases} 1 - p_{ji} & \text{if } \beta_{ij} = 1 \\ p_{ji} & \text{if } \beta_{ij} = 0 \end{cases}, \quad (29)$$

where p_{ji} is the SER in detection of x_j at U_i . Hence the probability of detecting x_j in state S_j is

$$Pr(S_j) = \prod_{i=j+1}^N G(\beta_{ij}). \quad (30)$$

Given a detection state S_j , we rewrite the conditional SINR in (28) for DAF WNC protocol as

$$\gamma_{j|S_j}^D = \frac{P_{jj}|h_{jd}|^2}{N_0} + \sum_{i=j+1}^N \frac{P_{ij}\beta_{ij}|h_{id}|^2}{r_{ij}N_0}, \quad (31)$$

where we have used $f_i = 1$ for DAF WNC protocol.

In general, the conditional SER for M-PSK modulation with conditional SNR γ for a generic set of channel coefficients $\{h_{uv}\}$ is given by [18]

$$p_{|\{h_{uv}\}} = \Psi(\gamma) \triangleq \frac{1}{\pi} \int_0^{(M-1)\pi/M} \exp\left(-\frac{b\gamma}{\sin^2 \theta}\right) d\theta, \quad (32)$$

where $b = \sin^2(\pi/M)$. Based on (18), the SNR, in detection of x_j at U_i , given the channel gain is $\gamma_{ji} = P_{jj}|h_{ji}|^2/N_0$. By averaging (32) with respect to the exponential random variable $|h_{ji}|^2$, the SER in detecting x_j at U_i can be shown as [18]

$$p_{ji} = F\left(1 + \frac{bP_{jj}\sigma_{ji}^2}{N_0 \sin^2 \theta}\right), \quad (33)$$

where

$$F(x(\theta)) = \frac{1}{\pi} \int_0^{(M-1)\pi/M} \frac{1}{x(\theta)} d\theta. \quad (34)$$

Given a detection state S_j , which can take $2^{(N-j)}$ values, the conditional SER in detecting x_j at the destination can be calculated using the law of total probability [19] as

$$p_{j|\{h_{id}\}_{i=j}^N}^D = \sum_{S_j=0}^{2^{(N-j)}-1} Pr(\hat{x}_j \neq x_j|S_j) \cdot Pr(S_j), \quad (35)$$

where $Pr(S_j)$ follows (30) and

$$Pr(\hat{x}_j \neq x_j|S_j) = \Psi\left(\gamma_{j|S_j}^D\right) \quad (36)$$

with $\gamma_{j|S_j}^D$ following (31). By averaging (35) with respect to the exponential random variables $\{|h_{id}|^2\}_{i=j}^N$, the exact SER in detecting x_j at the destination can be given by [5]

$$p_j^D = \sum_{S_j=0}^{2^{(N-j)}-1} F\left(\left(1 + \frac{bP_{jj}\sigma_{jd}^2}{N_0 \sin^2 \theta}\right) \prod_{i=j+1}^N \left(1 + \frac{bP_{ij}\beta_{ij}\sigma_{id}^2}{r_{ij}N_0 \sin^2 \theta}\right)\right) \prod_{i=j+1}^N G(\beta_{ij}), \quad (37)$$

where $G(\cdot)$ and $F(\cdot)$ follow (29) and (34), respectively.

Our next objective is to obtain the asymptotic SER performance, i.e., performance at high SNR, in detecting x_j at the destination. A number of approximations are needed. First, we expect that SER p_{ji} is sufficiently small compared to 1 at high SNR. Thus we assume that $(1 - p_{ji}) \simeq 1$ and rewrite (37) as

$$p_j^D \simeq \underbrace{\sum_{S_j=0}^{2^{(N-j)}-1} F\left(\left(1 + \frac{bP_j\alpha_{jj}\sigma_{jd}^2}{N_0 \sin^2 \theta}\right) \prod_{\substack{i=j+1 \\ \beta_{ij}=1}}^N \left(1 + \frac{bP_j\alpha_{ij}\sigma_{id}^2}{r_{ij}N_0 \sin^2 \theta}\right)\right)}_{\mathcal{A}} \underbrace{\prod_{\substack{i=j+1 \\ \beta_{ij}=0}}^N F\left(1 + \frac{bP_j\alpha_{jj}\sigma_{ji}^2}{N_0 \sin^2 \theta}\right)}_{\mathcal{B}}, \quad (38)$$

where $\alpha_{ij} = \frac{P_{ij}}{P_j}$ denotes the fraction of power P_j allocated at U_i in forwarding x_j . Secondly, because of high SNR, we can ignore the 1's in the argument of $F(\cdot)$. Let Ω_{j0} and Ω_{j1} denote subsets of the indices of mobile units that decode x_j erroneously and correctly, respectively. Then $\Omega_{j0} = \{i : \beta_{ij} = 0\}$ and $\Omega_{j1} = \{i : \beta_{ij} = 1\}$. Furthermore, $|\Omega_{j0}|$ and $|\Omega_{j1}| \in \{0, 1, \dots, (N - j)\}$, and $|\Omega_{j0}| + |\Omega_{j1}| = N - j$ for any detection state S_j , where $|\cdot|$ denotes the size of a set. Hence in (38), we can show that

$$\mathcal{A} \simeq \left(\frac{N_0}{bP_j} \right)^{1+|\Omega_{j1}|} \frac{g(1 + |\Omega_{j1}|)}{\alpha_{jj} \sigma_{jd}^2 \prod_{i \in \Omega_{j1}} \alpha_{ij} \frac{\sigma_{id}^2}{r_{ij}}}, \quad (39)$$

$$\mathcal{B} \simeq \left(\frac{N_0}{bP_j} \right)^{|\Omega_{j0}|} \frac{[g(1)]^{|\Omega_{j0}|}}{\alpha_{jj}^{|\Omega_{j0}|} \prod_{i \in \Omega_{j0}} \sigma_{ji}^2}, \quad (40)$$

where

$$g(x) = \frac{1}{\pi} \int_0^{(M-1)\pi/M} [\sin(\theta)]^{2x} d\theta. \quad (41)$$

Consequently, (38) can be rewritten as

$$p_j^D \simeq \left(\frac{bP_j}{N_0} \right)^{-(N-j+1)} \frac{1}{\sigma_{jd}^2} \sum_{S_j=0}^{2^{(N-j)}-1} \frac{g(1 + |\Omega_{j1}|) [g(1)]^{|\Omega_{j0}|}}{\alpha_{jj}^{1+|\Omega_{j0}|} \prod_{i \in \Omega_{j1}} \alpha_{ij} \left(\frac{\sigma_{id}^2}{r_{ij}} \right) \prod_{i \in \Omega_{j0}} \sigma_{ji}^2}. \quad (42)$$

The diversity order of a communication scheme is defined as

$$div = - \lim_{\gamma \rightarrow \infty} \frac{\log p(\gamma)}{\log \gamma}, \quad (43)$$

where $p(\gamma)$ is the SER associated with the SNR $\gamma \triangleq P_j/N_0$. From (42) and (43), the interference impact r_{ij} does not affect the diversity gain, and it is clear that x_j achieves full spatial diversity with an order of $N - j + 1$. Hence DAF WNC protocol provides the incremental diversity to the network, as expected.

Now when $j = N$, because x_N is directly transmitted to d , the exact and the asymptotic SER can be given by

$$p_N^D = F \left(1 + \frac{bP_N \sigma_{Nd}^2}{N_0 \sin^2 \theta} \right), \quad (44)$$

and

$$p_N^D \simeq \left(\frac{bP_N}{N_0} \right)^{-1} \frac{g(1)}{\sigma_{Nd}^2}, \quad (45)$$

respectively, where $F(\cdot)$ and $g(\cdot)$ follow (34) and (41), respectively.

For AAF WNC protocol, the conditional SER is

$$p_j^A_{|\{h_{id}, h_{ji}\}} = \Psi(\gamma_j^A), \quad (46)$$

where $\Psi(\cdot)$ is defined in (32) and γ_j^A follows (28) with f_i in (17) for AAF protocol.

4.2 Performance Validation of WNC Protocols

In this subsection, we perform computer simulations to validate the SER performance analysis for both DAF and AAF WNC protocols. The exact and asymptotic SER expressions in (37) and (42) are used for analytical results in DAF WNC protocol. For AAF WNC protocol, (46) is used to provide numerical results.

For simulation setup, BPSK modulation is used. The number of mobile units is $N = 4$, and the variance of the noise is $N_0 = 1$. We assume unit channel variances, i.e., $\sigma_{jd}^2 = \sigma_{ji}^2 = 1$ for $j = 1, \dots, N$ and $i = j + 1, \dots, N$ and transmit power $P_j = \sum_{i=j}^N P_{ij}$ corresponding to x_j is the same for all j . Furthermore, we assume equal power allocation [5] for x_j for $j = 1, \dots, N - 1$, i.e.

$$P_{ij} = \begin{cases} \frac{P_j}{2} & \text{if } i = j \\ \frac{P_j}{2(N-j)} & \text{if } j < i \leq N \end{cases} \quad (47)$$

since this strategy is optimal in the case of lacking channel state information at transmitters. For x_N , $P_{NN} = P_N$ since it is transmitted directly to the destination. We also assume that the cross-correlation $\rho_{ji} = \rho$ for all $i \neq j$, and we use $\rho = 0$ and $\rho = 0.5$ in our simulations. The mobile units are numbered in the decreasing order of their distance to the destination; therefore, we expect a diversity order of 4, 3, 2, and 1 for x_1 , x_2 , x_3 , and x_4 , respectively.

Figures 3 and 4 present the SER performance for DAF and AAF WNC protocols. In each figure, SER versus SNR (P_j/N_0) for each information x_j is presented. It is clear from the figures that WNC provides the expected diversity orders in both DAF and AAF protocols. In other words, using nonorthogonal code, WNC still achieves full diversity as shown in (42) for the case of DAF protocol. In addition, the figures show that for the case of $\rho = 0.5$, the gap at high SNR between orthogonal and nonorthogonal code is about 1dB, given the same SER.

5 Aggregate Transmit Power, Power Distribution, and Delay

In this section, we derive the expressions of aggregate transmit power and power distribution in a network at high SNR for the four considered schemes DTX, INC, MAX, and WNC. We also provide

the transmission delay for each scheme. These expressions are used to provide performance evaluation of INC, MAX, and WNC in the next section.

We consider a network consisting of N mobile units and a destination as described in Section 2, where transmissions from mobile units to a common destination are subject to TDMA and the same QoS represented by a SER p_0 . BPSK modulation is assumed for the demonstration purpose. For cooperation-based schemes INC, MAX, and WNC, we consider DAF protocol with equal power distribution strategy. Power P_j to transmit x_j is equally distributed between U_j and U_{j+1} in INC. For MAX and WNC, power P_j distributed among U_j, U_{j+1}, \dots, U_N follows (47).

5.1 DTX

In DTX, each mobile unit U_j directly transmits its information to d . The asymptotic SER expression for BPSK modulation can be given by [20]

$$p_j \simeq \frac{N_0}{4\sigma_{jd}^2 P_j}, \quad (48)$$

where N_0 is the variance of AWGN, P_j is the transmit power, and $\sigma_{jd}^2 = d_j^{-\alpha}$ is the variance of channel fading between U_j and d with the path loss exponent α . Consequently, given SER p_0 , transmit power associated with mobile unit U_j is

$$P_j \simeq \frac{N_0}{4\sigma_{jd}^2 p_0}, \quad (49)$$

and aggregate transmit power for DTX is

$$P_{DTX} = \sum_{j=1}^N P_j. \quad (50)$$

Because transmission from each mobile unit requires one time slot, transmission delay in DTX is N time slots for a network of N mobile units.

5.2 INC and MAX

INC and MAX apply two-user cooperative communication [4] and multi-node cooperative communication [5] in a network, respectively. Note that two-user cooperative communication is a specific case of multi-node cooperative communication [5]. Multi-node cooperative communication considers

a problem of single source s transmitting its information to a destination d with the assistance of \mathcal{N} relays $u_1, u_2, \dots, u_{\mathcal{N}}$. The asymptotic SER for M-PSK modulation can be expressed as [5]

$$p_{SER} \simeq \left(\frac{N_0}{bP}\right)^{\mathcal{N}+1} \frac{1}{\sigma_{sd}^2} \sum_{n=1}^{\mathcal{N}+1} \frac{g(\mathcal{N}-n+2) [g(1)]^{(n-1)}}{\alpha_s^n \prod_{l=n}^{\mathcal{N}} \alpha_{u_l} \sigma_{u_l d}^2 \prod_{k=1}^{n-1} \sigma_{su_k}^2}, \quad (51)$$

where b and $g(\cdot)$ are defined in Section 4.1, N_0 is the variance of AWGN, P is the transmit power, α_s and α_{u_n} are the fraction of transmit power P allocated at source s and relay u_n , respectively, and σ_{uv}^2 for generic nodes u and v is the channel variance of the link between u and v .

For BPSK modulation ($M = 2$), we can show that $b = 1$ and $g(x) = \frac{1}{2\sqrt{\pi}} \cdot \frac{\Gamma(\frac{1}{2}+x)}{\Gamma(1+x)}$, where $\Gamma(\cdot)$ is the Gamma-function. Because x takes integer values in (51), we can further show that $\Gamma(\frac{1}{2} + x) = \sqrt{\pi} \cdot \frac{(2x-1)!!}{2^x}$ and $\Gamma(1+x) = x!$, where $(\cdot)!$ and $(\cdot)!!$ are single factorial and double factorial operations, respectively. If we consider equal power allocation strategy, then the SER for detecting the source information is given by

$$p_{SER} \simeq \left(\frac{N_0}{P}\right)^{\mathcal{N}+1} \frac{1}{\sigma_{sd,\text{eff}}^2}, \quad (52)$$

where

$$\sigma_{sd,\text{eff}}^2 = \frac{\sigma_{sd}^2}{\sum_{n=1}^{\mathcal{N}+1} \frac{(2(\mathcal{N}-n+2)-1)!!}{(\mathcal{N}-n+2)!} \cdot \frac{\mathcal{N}^{\mathcal{N}-n+1}}{2^n \prod_{l=n}^{\mathcal{N}} \sigma_{u_l d}^2 \prod_{k=1}^{n-1} \sigma_{su_k}^2}} \quad (53)$$

is the effective channel variance between the source and the destination in \mathcal{N} -relay multi-node cooperative communication. From (52), the transmit power for a given SER p_0 at high SNR is

$$P \simeq N_0 (p_0 \sigma_{sd,\text{eff}}^2)^{-\frac{1}{\mathcal{N}+1}}. \quad (54)$$

For two-user cooperative communication, (52)-(54) can be applied directly with $\mathcal{N} = 1$. It can also be shown that

$$\sigma_{sd,\text{eff}}^2 = 4\sigma_{sd}^2 \left(\frac{1}{\sigma_{su}^2} + \frac{3}{\sigma_{ud}^2} \right)^{-1}, \quad (55)$$

where u denotes the relay unit.

Given the network in Section 2 that consists of N mobile units U_1, U_2, \dots, U_N transmitting their information x_1, x_2, \dots, x_N , respectively, to a common destination, multi-node cooperative communication is applied in MAX as follows. MAX comprises of $(N - 1)$ multi-node cooperative communication stages and a direct transmission stage. The j th cooperation stage involves a source node U_j and $\mathcal{N} = N - j$ relays, which are mobile units U_{j+1}, \dots, U_N located between U_j and d . Thus diversity

orders of $N, (N-1), \dots, 2$ are expected for U_1, \dots, U_{N-1} , respectively. The effective channel variance between U_j and d , $\sigma_{jd,\text{eff}}^2$, can be directly determined using (53) with $\mathcal{N} = N - j$. Consequently, given SER p_0 , transmit power P_j associated with x_j follows (54) with $\sigma_{sd,\text{eff}}^2 = \sigma_{jd,\text{eff}}^2$ and $\mathcal{N} = N - j$. The power P_j is distributed among U_j, U_{j+1}, \dots, U_N following the equal power distribution strategy in (47). Mobile unit U_N operates in direct transmission mode with diversity order of one and transmit power $P_{NN} = P_N$ following (49). Because U_i for $i = 1, \dots, N$ forwards x_1, x_2, \dots, x_{i-1} and transmits its own x_i to the destination, transmit power required at U_i is

$$P_i^{\text{MAX}} = \sum_{j=1}^i P_{ij}. \quad (56)$$

Thus aggregate transmit power for MAX is

$$P_{\text{MAX}} = \sum_{i=1}^N P_i^{\text{MAX}} = \sum_{i=1}^N \sum_{j=1}^i P_{ij}. \quad (57)$$

Similarly, INC consists of $(N-1)$ two-user cooperative communication stages for U_1, \dots, U_{N-1} and one direct transmission stage for U_N . The effective channel variance between U_j and d , $\sigma_{jd,\text{eff}}^2$, for $j = 1, \dots, (N-1)$ can be determined based on (55). From that, given SER p_0 , transmit power P_j associated with x_j is determined by (54) where $\mathcal{N} = 1$. The power P_j is divided equally between U_j and U_{j+1} . U_N operates in direct transmission mode with transmit power $P_{NN} = P_N$ following (49). Because U_i forwards x_{i-1} and transmits its own x_i , transmit power at U_i is

$$P_i^{\text{INC}} = \frac{(P_{(i-1)} + P_i)}{2}. \quad (58)$$

Thus aggregate transmit power for INC is

$$P_{\text{INC}} = \sum_{i=1}^N P_i^{\text{INC}} = \sum_{i=1}^N \frac{(P_{(i-1)} + P_i)}{2}. \quad (59)$$

In INC and MAX, each relay requires one time slot for its transmission. Thus transmission delay in INC and MAX is $(2N-1)$ and $N(N+1)/2$ time slots, respectively. The transmission delay in INC grows linearly with the network size while that in MAX grows quadratically.

5.3 WNC

From (42), following the same procedure in Section 5.2 for BPSK modulation, we are able to show that

$$p_j^D \simeq \left(\frac{N_0}{P_j} \right)^{N-j+1} \frac{1}{\sigma_{jd,\text{eff}}^2} \quad (60)$$

for $j = 1, \dots, (N-1)$, where

$$\sigma_{jd,\text{eff}}^2 = \frac{\sigma_{jd}^2}{\sum_{S_j=0}^{2^{(N-j)}-1} \frac{(2|\Omega_{j1}|+1)!!}{(1+|\Omega_{j1}|)!} \cdot \frac{(N-j)^{|\Omega_{j1}|}}{2^{1+|\Omega_{j0}|} \prod_{i \in \Omega_{j1}} \frac{\sigma_{id}^2}{r_{ij}} \prod_{i \in \Omega_{j0}} \sigma_{ji}^2}} \quad (61)$$

is the effective channel variance between U_j and d . From (60), given SER p_0 , transmit power associated with x_j is

$$P_j \simeq N_0 (p_0 \sigma_{jd,\text{eff}}^2)^{-\frac{1}{N-j+1}}. \quad (62)$$

Equal power distribution strategy is also used in WNC where P_j is distributed following (47). Mobile unit U_N operates in direct transmission mode with transmit power $P_{NN} = P_N$ following (49). Because U_i for $i = 1, \dots, N$ forwards x_1, x_2, \dots, x_{i-1} and transmits its own x_i to the destination, transmit power at U_i is

$$P_i^{\text{WNC}} = \sum_{j=1}^i P_{ij}. \quad (63)$$

Thus aggregate transmit power for WNC is

$$P_{\text{WNC}} = \sum_{i=1}^N P_i^{\text{WNC}} = \sum_{i=1}^N \sum_{j=1}^i P_{ij}. \quad (64)$$

Based on WNC transmission structure in Section 2, transmission delay in WNC is $(2N-1)$ time slots.

6 Performance Simulation and Validation

In this section, we perform computer simulations to evaluate and validate INC, MAX, and WNC performance. We aim to verify that these schemes result in substantial reduction of aggregate transmit power over DTX and to confirm that WNC achieves low aggregate transmit power and even power distribution with low transmission delay. To show power reduction of scheme 2 over scheme 1, we

define

$$\text{Power reduction} = \frac{P_{\text{scheme1}} - P_{\text{scheme2}}}{P_{\text{scheme1}}} \times 100(\%). \quad (65)$$

For simulation setup, we assume a network whose N mobile units are uniformly distributed in an area $\mathcal{A} = [0, 2]^2$ and the destination locates at $(0, 0)$ as shown in Figure 1. We consider the path loss exponent $\alpha = 3$, the SER $p_0 = 5 \times 10^{-4}$, and the noise variance $N_0 = 10^{-2}$. The results are obtained over 1000 network realizations. For each network realization, we compute channel variances between any two nodes u and v as $\sigma_{uv}^2 = d_{uv}^{-\alpha}$ where d_{uv} is the distance between the two nodes.

6.1 Validation of INC, MAX, and WNC Improvement over DTX

Figure 5 presents the reduction in aggregate transmit power using INC, MAX, and WNC over DTX for various network sizes. For WNC, we take the cross-correlation $\rho = 0.5$. It is clear from the figure that great reduction in aggregate transmit power can be achieved using INC, MAX, and WNC over DTX, especially for large network sizes. The power reduction of 69% at a network size of two increases rapidly as the network size increases and achieves more than 90% for network sizes larger than five mobile units. The reason for INC, MAX, and WNC achieving substantial power reduction is the spatial diversity used to compensate the large path loss. Mobile units other than U_N in INC receive a diversity order of two for their transmission while those in MAX and WNC receive diversity order incrementally based on their locations. The spatial diversity results in substantial reduction of the aggregate transmit power in our schemes over DTX.

Figure 6 presents the distribution of aggregate transmit power in a 10-unit network for the four considered schemes; nevertheless, the finding is unique to other network sizes. Note that mobile units are numbered in the decreasing order of their distance to the destination. Clearly from the figure, DTX leads to substantial power burden on mobile units away from the destination. This is due to large transmit powers required in association with large distances. The power burden reduction in INC is due to diversity order of two for each mobile unit and transmit power shared by two consecutive units, a half of power for each. High transmit power for distant units, however, still remains. Nevertheless, power distribution is much better than that in DTX as shown in the figure. The best power distribution is found in MAX and WNC. In these schemes, incremental diversity provides higher diversity order to mobile units with larger distances to compensate the high required

transmit power. Furthermore, the higher transmit power is shared by the larger group of mobile units. Consequently, MAX and WNC achieve the best power distribution as shown in the figure.

6.2 Validation of WNC over INC and MAX

It is clear from Figures 5 and 6 that WNC for the case of $\rho = 0.5$ results in a comparable performance with MAX. In particular, Figure 5 shows that power reduction of WNC over DTX is less than 1% lower than that of MAX while Figure 6 reveals that WNC and MAX have the same power distribution profile.

Now let us take a close look at INC, MAX, and WNC performance. Figure 7 illustrates the aggregate transmit power using INC, MAX, and WNC in a 10-unit network for various values of the cross correlation ρ ; nevertheless, the finding is unique for other network sizes. As shown in the figure, when ρ is chosen appropriately, for example $\rho \in [0, 0.6]$ in this setup, aggregate transmit power in WNC and MAX is not much different. It is also clear from the figure that WNC outperforms INC in terms of aggregate transmit power for a wide range of ρ values ($\rho \in [0, 0.85]$ in this setup) and WNC performance becomes no longer better than INC only for very high values of ρ ($\rho > 0.85$ in this setup). Here high values of the cross correlation ρ associate with high interference, caused by the linear combination of overheard symbols at relay, that overcomes the benefit of incremental diversity and causes high aggregate transmit power in WNC.

Lastly, Figure 8 provides the power distribution among mobile units using INC, MAX, and WNC for various values of ρ for the same network in Figure 7. We see that WNC provides the same power distribution profile as MAX for any $\rho \leq 0.9$. Moreover, WNC outperforms INC in terms of power distribution for a wide range of ρ values. Even for $\rho = 0.95$, WNC power distribution profile is still better than that of INC (the node power varies within 2 units in WNC while that is about 3.5 in INC) although WNC with this ρ value results in much higher aggregate transmit power as shown in Figure 7. Incremental diversity in WNC, where higher diversity order are allocated for more distant mobile units to reduce the high transmit power, provides the balance in power distribution. Furthermore, transmit power is shared among many mobile units by cooperative communication, where higher transmit power is shared by a larger group of relays, providing further balance in power distribution.

6.3 Remarks

From the performance evaluation presented in this section, a number of remarks are noteworthy. First, the jump in transmit power at U_N , the closest mobile unit to the destination, in INC, MAX, and WNC in Figures 6 and 8 is due to the fact that this unit does not receive assistance from others and the transmission of its own information is in direct mode. Also the most distant unit U_1 may require less transmit power than others in INC and WNC since it is not required to assist any unit. Second, as we have seen, INC, MAX, and WNC outperform DTX greatly in terms of aggregate transmit power and power distribution. Higher gain in power reduction and even power distribution of INC, MAX, and WNC over DTX is expected when higher QoS, equivalently lower SER, is desired. A similar notice is given for the case of using MAX and WNC over INC. Third, MAX achieves the lowest power aggregation and the best power distribution, as shown in Figures 5 - 8. However, the transmission delay in MAX is very high, compared to WNC and INC, as illustrated in Figure 9. For a network of N mobile units, MAX incurs a delay of $N(N+1)/2$ time slots while both WNC and INC have the same transmission delay of $(2N-1)$ time slots. On the other hand, although INC incurs a low transmission delay, it requires much higher transmit power and the power is distributed unevenly, as revealed in Figures 6 and 8. Clearly, WNC achieves the advantages of both MAX and INC, which are characterized by low transmit power, even power distribution, and low transmission delay. Lastly, WNC requires no multiuser detection at mobile units while it employs a simple multiuser detection method at the destination, as shown in Section 3. These characteristics make WNC be the best candidate to improve network performance.

7 Conclusions

In this paper, we have considered a number of location-aware cooperation-based schemes, namely immediate-neighbor cooperation (INC), maximal cooperation (MAX), and wireless network cocast (WNC) that achieve spatial diversity to reduce aggregate transmit power and achieve even power distribution in a network. INC utilizes two-user cooperative communication in a network, resulting in good reduction of aggregate transmit power; however, the issue of uneven power distribution still remains. MAX utilizes multi-node cooperative communication, providing incremental diversity to

solve the uneven power distribution and achieves substantial reduction in aggregate transmit power. However, transmission delay in MAX grows quadratically with the network size. For a network of N mobile units, the transmission delays in INC and MAX are $(2N - 1)$ and $N(N + 1)/2$ time slots, respectively. The novel WNC utilizes cocast to resolve the weaknesses of INC and MAX. In particular, INC, MAX, and WNC can result in more than 90% reduction in aggregate transmit power over DTX. Moreover, WNC can achieve low aggregate transmit power and even power distribution of MAX with low transmission of INC.

References

- [1] K. J. R. Liu, A. K. Sadek, W. Su, and A. Kwasinski, *Cooperative Communications and Networking*. Cambridge University Press, 2008.
- [2] T. Himsoon, W. P. Siriwongpairat, Z. Han, and K. J. R. Liu, "Lifetime maximization via cooperative nodes and relay deployment in wireless networks," *IEEE J. Sel. Areas Commun., Specical Issue on Cooperative Communications and Networking*, vol. 25, no. 2, pp. 306–317, Feb. 2007.
- [3] J. N. Laneman, D. N. C. Tse, and G. W. Wornell, "Cooperative diversity in wireless networks: efficient protocols and outage behavior," *IEEE Trans. Inform. Theory*, vol. 50, no. 12, pp. 3062–3080, Dec. 2004.
- [4] W. Su, A. K. Sadek, and K. J. R. Liu, "Cooperative communications in wireless networks: performance analysis and optimum power allocation," *Wireless Personal Communications*, vol. 44, no. 2, pp. 181–217, Jan. 2008.
- [5] A. K. Sadek, W. Su, and K. J. R. Liu, "Multinode cooperative communications in wireless networks," *IEEE Trans. Signal Process.*, vol. 55, no. 1, pp. 341–355, Jan. 2007.
- [6] A. Ibrahim, A. K. Sadek, W. Su, and K. J. R. Liu, "Cooperative communications with partial channel state information: when to cooperate?," *Proc. IEEE GLOBECOM*, vol. 5, pp. 3068–3072, Nov. 2005.
- [7] A. Ibrahim, A. K. Sadek, W. Su, and K. J. R. Liu, "Cooperative communications with relay selection: when to cooperate and whom to cooperate with?," *IEEE Trans. Wireless Commun.*, vol. 7, no. 7, pp. 2814–2827, July 2008.
- [8] J. N. Laneman and G. W. Wornell, "Distributed space-time coded protocols for exploiting cooperative diversity in wireless networks," *IEEE Trans. Inform. Theory*, vol. 49, pp. 2415–2525, Oct. 2003.
- [9] Y. Cao and B. Vojcic, "MMSE multiuser detection for cooperative diversity CDMA systems," *Proc. IEEE WCNC*, vol. 1, pp. 42–47, Mar. 2004.
- [10] E. Larsson and B. R. Vojcic, "Cooperative transmit diversity based on superposition modulation," *IEEE Commun. Lett.*, vol. 9, no. 9, pp. 778–780, Sept. 2005.
- [11] L. Xiao, T. Fuja, J. Klierer, and D. Costello, "A network coding approach to cooperative diversity," *IEEE Trans. Info. Theory*, vol. 53, no. 10, pp. 3714–3722, Oct. 2007.
- [12] K. Ishii, "Cooperative transmit diversity utilizing superposition modulation," *Proc. IEEE Radio and Wireless Symposium*, pp. 337–340, Jan. 2007.

- [13] T. Bui and J. Yuan, "Iterative approaches of cooperative transmission based on superposition modulation," *Proc. IEEE ISCIT*, pp. 1423–1428, Oct. 2007.
- [14] L. Venturino, X. Wang, and M. Lops, "Multiuser detection for cooperative networks and performance analysis," *IEEE Trans. Signal Process.*, vol. 54, no. 9, pp. 3315–3329, Sept. 2006.
- [15] G. Sun, J. Chen, W. Guo, and K. J. R. Liu, "Signal processing techniques in network aided positioning: A survey," *IEEE Signal Process. Mag.*, vol. 22, no. 4, pp. 12–23, Jul. 2005.
- [16] A. H. Sayed, A. Tarighat, and N. Khajehnouri, "Network-based wireless location," *IEEE Signal Process. Mag.*, vol. 22, no. 4, pp. 24–40, Jul. 2005.
- [17] C. D. Meyer, *Matrix Analysis and Applied Linear Algebra*. USA: SIAM, 2000.
- [18] M. K. Simon and M. S. Alouini, "A unified approach to the performance analysis of digital communication over generalized fading channels," *Proc. IEEE*, vol. 86, no. 9, pp. 1860–1877, Sept. 1998.
- [19] A. Leon-Garcia, *Probability and Random Processes for Electrical Engineering*. USA: Addison Wesley Longman, 2nd ed., 1994.
- [20] J. G. Proakis, *Digital Communications*. NewYork, USA: McGraw-Hill, 4th ed., 2001.

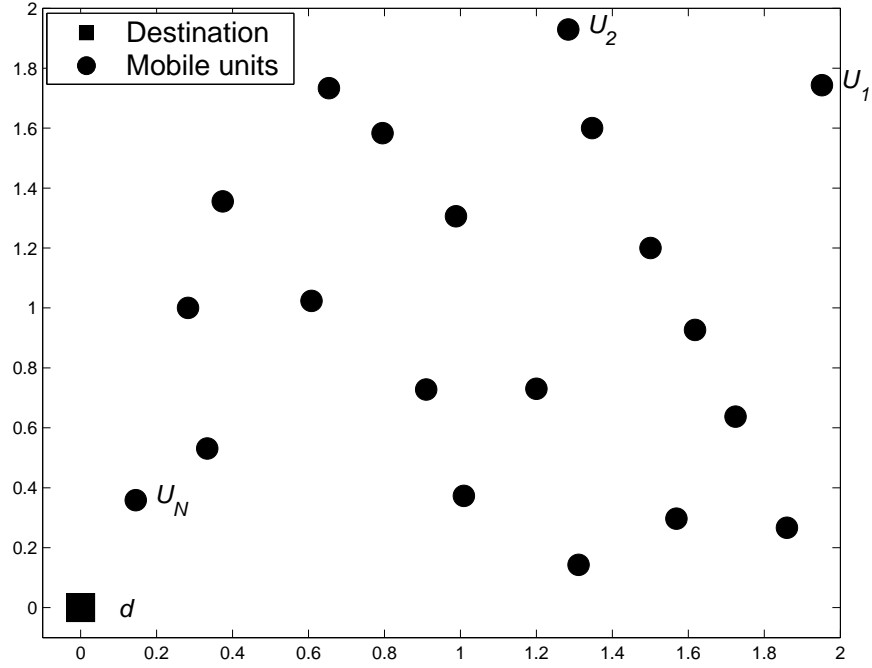


Figure 1: A uniformly distributed network with a destination d and N mobile units U_1, U_2, \dots, U_N numbered in decreasing order of their distance to the destination.

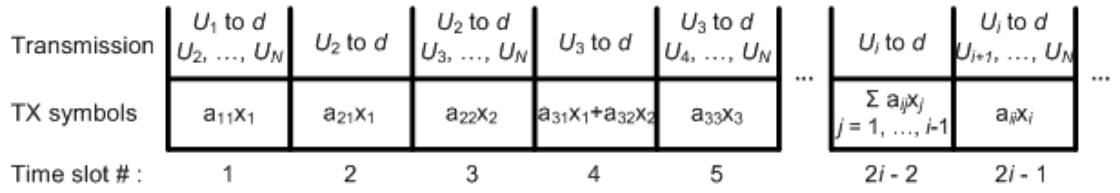


Figure 2: Wireless Network Cocast (WNC) - Transmission structure.

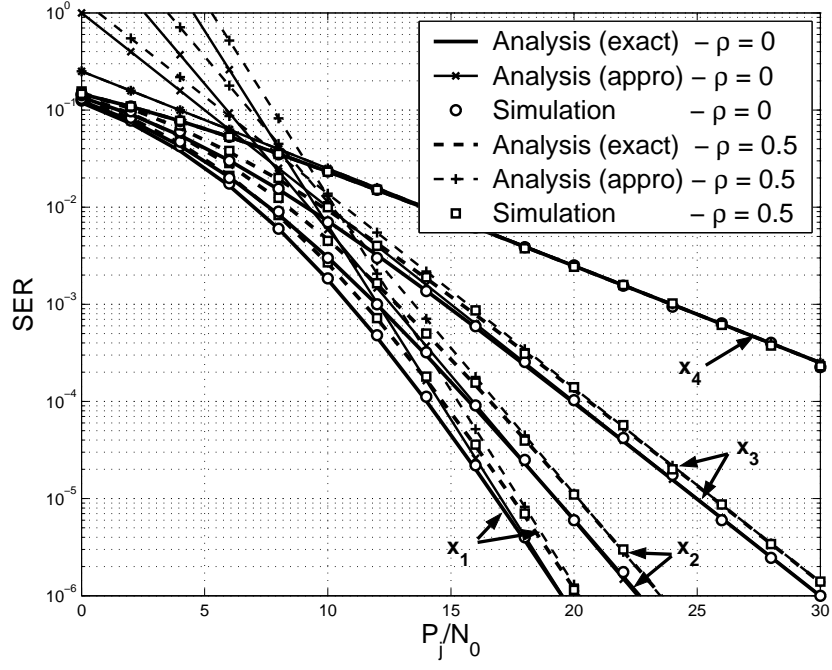


Figure 3: SER versus SNR performance for BPSK modulation in DAF WNC protocol.

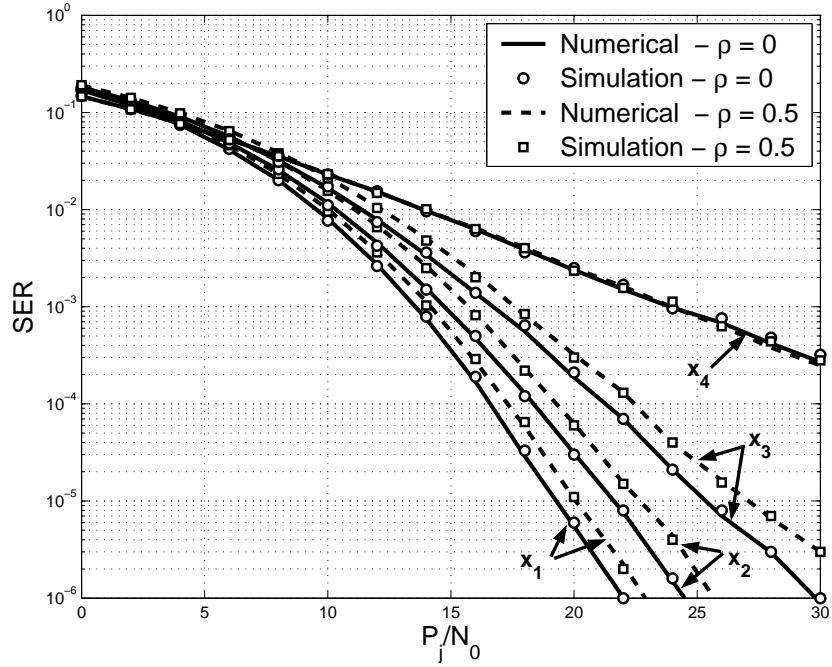


Figure 4: SER versus SNR performance for BPSK modulation in AAF WNC protocol.

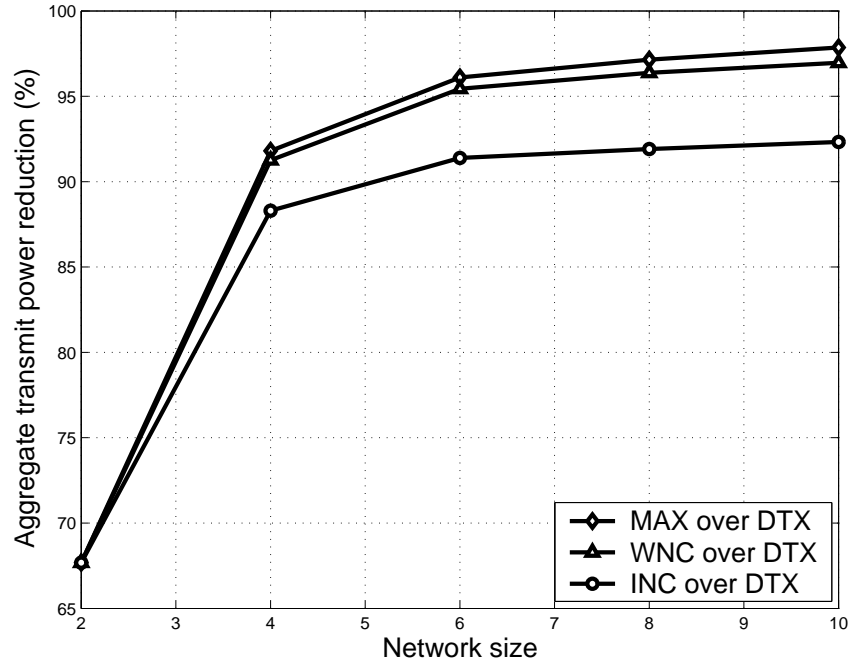


Figure 5: Reduction in aggregate transmit power of INC, MAX, and WNC ($\rho = 0.5$) over DTX versus network size.

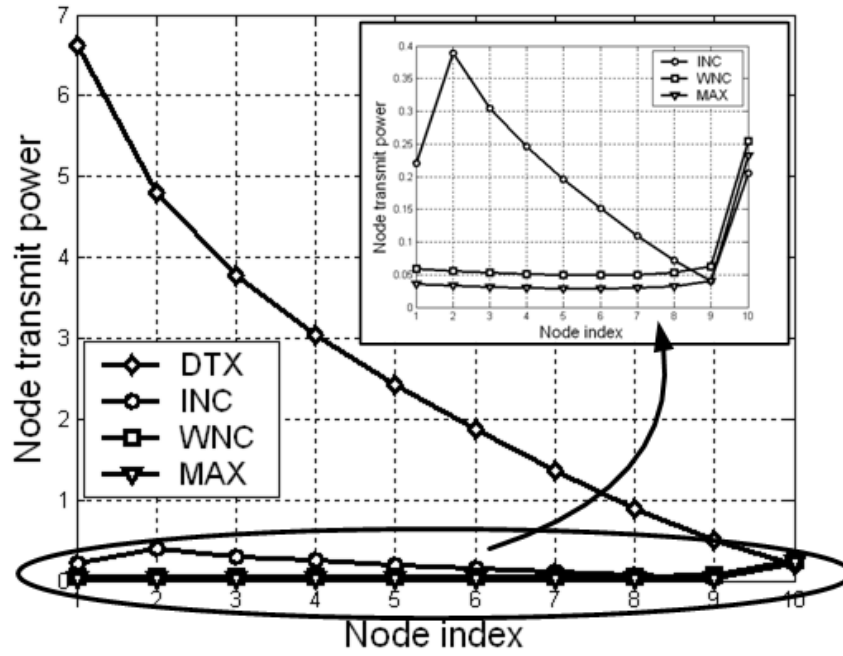


Figure 6: Distribution of transmit power in DTX, INC, MAX, and WNC ($\rho = 0.5$) for a 10-unit network.

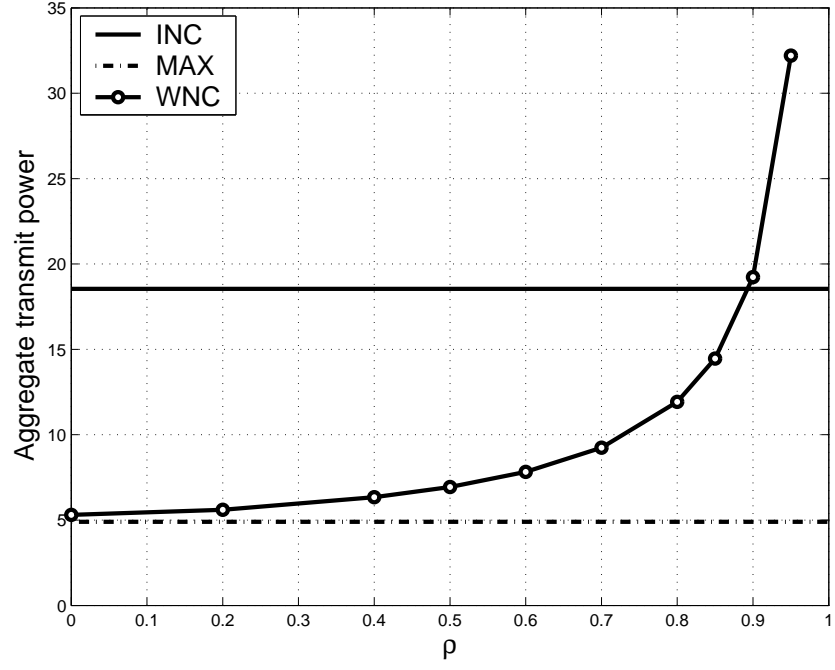


Figure 7: Aggregate transmit power in INC, MAX, and WNC versus ρ for a 10-unit network.

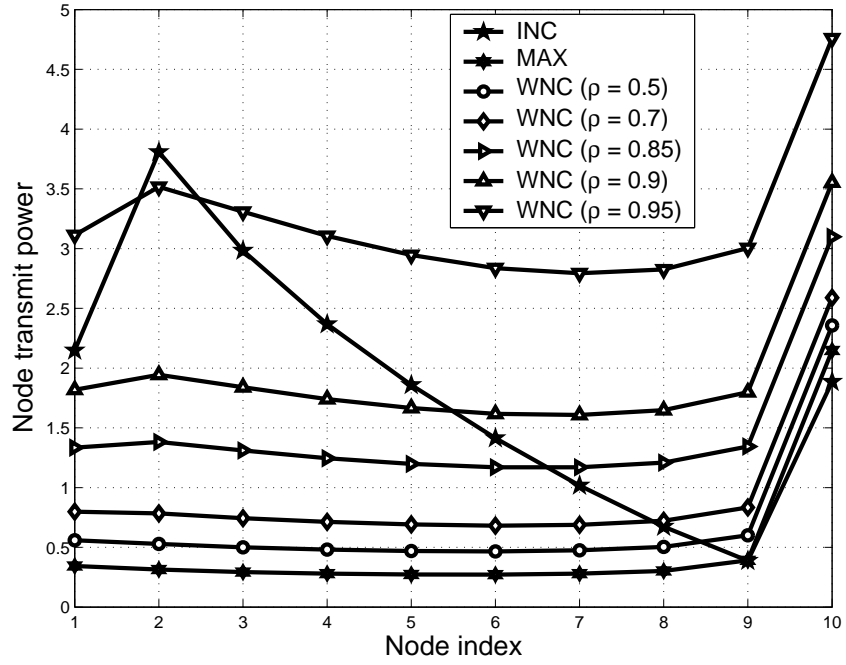


Figure 8: Power distribution in INC, MAX, and WNC (for various ρ values) for a 10-unit network.

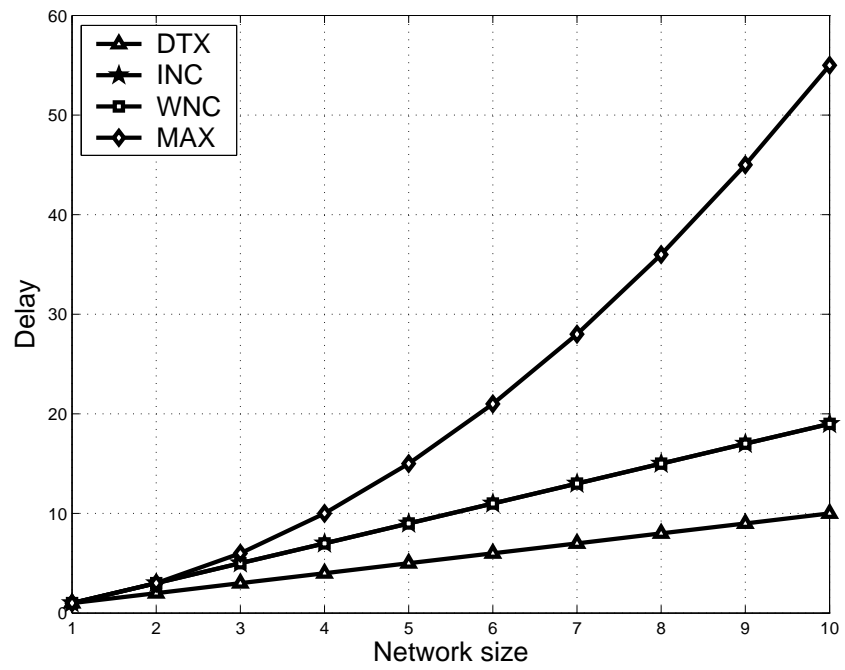


Figure 9: Transmission delay in DTX, INC, MAX, and WNC.